EUROPEAN COOPERATION
IN THE FIELD OF SCIENTIFIC
AND TECHNICAL RESEARCH

EURO-COST

COST 273 TD(05)096
Lisbon, Portugal
2005/Nov/10-11

SOURCE: Centre for Communications Research
University of Bristol
United Kingdom

A Quantification of 3-D Directional Spread from Small-Scale Fading Analysis

A. Pal, M. A. Beach and A. R. Nix
Centre for Communications Research
2.19 Merchant Venturers Building
Bristol, BS8 1UB, United Kingdom
Phone: +44 117 928 5202
Fax: +44 117 954 5206
Email: A.Pal@bris.ac.uk

A Quantification of 3D Directional Spread from Small-Scale Fading Analysis

Arindam Pal, Mark Beach and Andy Nix

Centre for Communications Research
University of Bristol, Bristol, United Kingdom
A.Pal@bris.ac.uk

***Abstract* – The terms "angular spread" and "multipath richness" are frequently used in literature in reference to the directional spread of the multipath energy arriving at the receiver. Although its magnitude is fundamental to the performance of spatial diversity antenna arrays, current literature falls short of providing a precise mathematical definition for directional spread when an arbitrary 3-D directional distribution is considered. In this paper, a quantification of directional spread that is applicable for arbitrary energy distributions of multipath rays/clusters in the 3-D directional domain has been proposed from analysis of second order statistics of small-scale fading. The proposed metrics overcome the limitations of the conventional RMS angular spread metric.**

I. Introduction

The statistics of small-scale fading is critical to inter-element correlation and ultimately the information theoretical capacity of Multiple-Input Multiple-Output (MIMO) channels employing space-diversity arrays [1]. Small-scale fading refers to the rapid fluctuation of received power over sub-wavelength distances in space, that is produced by scattered electromagnetic waves arriving from diverse directions. A higher rate and density of fading leads to decorrelation of spatially separated elements and improvement in MIMO capacity. It has been demonstrated that the standard deviation or the root-means-square (RMS) spread of the angular energy distribution is the dominating factor for determining correlation as opposed to the specific angular energy distribution function [2]. Although it is commonly used for characterisation of channels, the RMS angular spread metric is not sufficiently comprehensive or convenient. This is firstly because it must be stated separately for the azimuth and the elevation domains. Secondly, since the power azimuth spectrum is a periodic function, the conventional RMS measure is unsuitable for large angular separations and must be applied separately for each cluster when there are multiple well-spaced clusters [3]. A system of characterising angular spread that is applicable to arbitrary azimuth energy distributions was proposed in [4], but the analysis was limited only to the azimuth domain. An expression for 3-D directional spread was also proposed in [5], but its relation to fading statistics is not apparent.

Partly due to the lack of a simple metric that describes the 3-D directional energy spread, the concept of "multipath richness" is frequently used to characterise channels. It was observed that the notion of multipath richness is less formal than capacity and that there were several potential measures that could be used [6]. The term 'multipath richness' was used to define the number of independent resolvable paths propagating from the transmitter to the receiver [7][8], as increasing the number of antenna elements beyond this results in saturation of capacity. In [6], multipath richness was quantified using the effective degrees of freedom (EDOF) metric. EDOF is the slope of capacity versus signal-to-noise ratio (SNR) at one value of SNR and gives an indication of the rank of the system [9]. In addition, a relative sum of singular values of the channel response matrix [10] and the cumulative sum of the log of normalized eigenvalues [11] have also been proposed as metrics for multipath richness. These metrics are indicative of the fading statistics in the channel, but they are calculated from the MIMO channel response and therefore have a dependency on the array configuration. This is not ideal even if the arrays are as simplistic as Uniform Linear Arrays (ULA) or Uniform Circular Arrays (UCA) employing omnidirectional elements, as multipath richness is essentially a property of the channel. Thus, an alternative metric that is independent of the antenna specification is needed. An antenna independent metric would be useful for simulation-based evaluations of antenna array designs and signalling schemes under diverse multipath profiles.

In this paper, a quantification of the 3-D directional spread of a multipath energy distribution is proposed from an analysis of the second order statistics of small-scale fading. The proposed metrics give an indication of the information theoretical capacity that can be expected for MIMO systems employing spatial diversity antennas. Concise definitions that are dependant only on the parameters of multipath components (in the format commonly obtainable from 3-D ray-tracing models), i.e., powers and 3-D directions, have been derived for the proposed metrics.

II. Theoretical Analysis

A. Directional Derivatives of the Fading Function

The rate of fluctuation of the spatially fading stationary process is given by the first order spatial derivative of the received voltage, received power or received envelope. The analysis in this paper has been done for received power, which is denoted for a point in space $\mathbf{s} = [x, y, z]$ as $f(x, y, z)$. The vector representing the first order partial derivatives is given by $\nabla f = [f_x, f_y, f_z]$. The rate of variation of $f(x, y, z)$ in a given direction $\mathbf{u}$ is given by the three-dimensional directional derivative of $f(x, y, z)$, and is denoted as $m_{\mathbf{u}}$. The directional

Arindam Pal would like to thank ORS UK and the University of Bristol for the postgraduate scholarship.

unit vector $\hat{\mathbf{u}}$ is defined in Cartesian and spherical co-ordinates as

$$\hat{\mathbf{u}} = \begin{bmatrix} u_x \\ u_y \\ u_z \end{bmatrix} = \begin{bmatrix} \sin\theta\cos\varphi \\ \sin\theta\sin\varphi \\ \cos\theta \end{bmatrix} \quad (1)$$

where (θ,φ) represent the spherical co-ordinate angles. $\mathrm{m}_\mathbf{u}$ is given by (2).

$$\begin{aligned} \mathrm{m}_\mathbf{u} &= \nabla_\mathbf{u} f = \nabla f \cdot \frac{\mathbf{u}}{|\mathbf{u}|} \\ &= \lim_{l\to 0} \frac{f(\mathbf{x}+l\hat{\mathbf{u}}) - f(\mathbf{x})}{l} \\ &= \frac{\partial f}{\partial x} u_x + \frac{\partial f}{\partial y} u_y + \frac{\partial f}{\partial z} u_z \\ &= f_x u_x + f_y u_y + f_z u_z \end{aligned} \quad (2)$$

The mean of $\mathrm{m}_\mathbf{u}$ taken over many realisations of independent multipath phases must be zero. The mean square or the second order moment of $\mathrm{m}_\mathbf{u}$, denoted as $\sigma_\mathrm{m}^2(\hat{\mathbf{u}})$, is the statistic that gives a measure of the fading rate in the direction $\mathbf{u}$ as is given by

$$\begin{aligned} \sigma_\mathrm{m}^2(\hat{\mathbf{u}}) = E\{\mathrm{m}_\mathbf{u}{}^2\} = \mathrm{E}\{f_x^2\}u_x^2 + \mathrm{E}\{f_y^2\}u_y^2 + \mathrm{E}\{f_z^2\}u_z^2 + \mathrm{E}\{f_x f_y\}u_x u_y + \\ + \mathrm{E}\{f_y f_z\}u_y u_z + \mathrm{E}\{f_z f_x\}u_z u_x \end{aligned} \quad (3)$$

where the second order moments of the partial derivatives are denoted as follows:

$$\begin{aligned} &R_{xx} = \mathrm{E}\{f_x^2\} \quad R_{yy} = \mathrm{E}\{f_y^2\} \quad R_{zz} = \mathrm{E}\{f_z^2\} \\ &R_{xy} = \mathrm{E}\{f_x f_y\} \quad R_{yz} = \mathrm{E}\{f_y f_z\} \quad R_{zx} = \mathrm{E}\{f_z f_x\} \end{aligned} \quad (4)$$

The $\sigma_\mathrm{m}^2(\hat{\mathbf{u}})$ describes the second order statistics of small-scale fading at any point in space as a function of direction emanating from the point. In order to estimate $\sigma_\mathrm{m}^2(\hat{\mathbf{u}})$ efficiently, simple expressions are needed for R_{xx}, R_{yy}, R_{zz}, R_{xy}, R_{yz} and R_{zx}. Expressions for (f_x, f_y, f_z) and their covariances are derived in Section II.*B*.

B. *Covariance of Partial Derivatives*

The power of a spatially fading stationary wave is given by $f = |h|^2$, where h is the normalised channel response given by the summation of N_s multipath waves. The assumption that electromagnetic radiation arrives at the receiver in planar wavefronts will be used. Denoting the direction of arrival as a vector ($\mathbf{d} = [d_x, d_y, d_z]$), h is given by

$$h = \sum_{s=1}^{N_s} A_s \exp\left(i\left(\hat{\mathbf{d}}_s \cdot \mathbf{s} + \chi_s\right)\right) = \sum_{s=1}^{N_s} A_s \exp(i\psi_s) \quad (5)$$

where ψ_s denotes the overall phase of the sth multipath ray and A_s^2 is power of each ray after normalization so that the total power equals unity. The expressions for the partial derivatives are shown for the case of f_x.

$$f_x = \frac{\partial |h|^2}{\partial x} = h^* \frac{\partial h}{\partial x} + h\frac{\partial h^*}{\partial x} = 2\,\mathrm{Re}\left\{\frac{\partial h}{\partial x} h^*\right\} \quad (6)$$

$$\frac{\partial h}{\partial x} = \sum_{s=1}^{N_s} A_s i d_{x_s} \exp(i\psi_s) \quad (7)$$

Using (5), (6) and (7), and ignoring the multiplication factor of 2 in (6), f_x simplifies to a summation of a large number of independent and identically distributed (i.i.d) random variables, as shown in (8). The central limit theorem dictates that f_x, f_y and f_z are gaussian distributed.

$$\begin{aligned} f_x &= \mathrm{Re}\left\{\sum_{s=1}^{N_s} A_s i d_{x_s} \exp(i\psi_s) \cdot \sum_{k=1}^{N_s} A_k \exp(-i\psi_k)\right\} \\ &= \sum_{s=1}^{N_s}\sum_{k=1}^{N_s} A_s A_k d_{x_s} \sin(\psi_s - \psi_k) \\ &= \sum_{s=1}^{N_s}\sum_{k=1}^{s} A_s A_k \left(d_{x_s} - d_{x_k}\right)\sin(\psi_s - \psi_k) \end{aligned} \quad (8)$$

A derivation of the general expression for the second order moment of the partial derivatives, as given by (9), is shown in Appendix A.

$$R_{xy} = \frac{1}{2}\sum_{s}^{N_s} A_s^2 \left(d_{x_s} - \bar{d}_x\right)\left(d_{y_s} - \bar{d}_y\right) \quad (9)$$

More specifically, the variance in any co-ordinate direction is given by the energy spread of the directional components resolved in that direction, as shown in (10).

$$R_{xx} = \frac{1}{2}\sum_{s}^{N_s} A_s^2 \left(d_{x_s} - \bar{d}_x\right)^2 \quad (10)$$

In (9) and (10), $\bar{d}_x$ and $\bar{d}_y$ are components of $\bar{\mathbf{d}}$ where

$$\bar{\mathbf{d}} = \sum_{s=1}^{N_s} A_s^2 \mathbf{d}_s = \sum_{s=1}^{N_s} A_s^2 \left(d_{x_s}\hat{\mathbf{i}} + d_{y_s}\hat{\mathbf{j}} + d_{z_s}\hat{\mathbf{k}}\right) = \bar{d}_x\hat{\mathbf{i}} + \bar{d}_y\hat{\mathbf{j}} + \bar{d}_z\hat{\mathbf{k}}. \quad (11)$$

The expressions in (9) and (10) take a similar form as the general expressions for covariance and variance respectively, except that the directional components here are weighted by the powers of the mulitpath components instead of probabilities. There is no phase dependency as they are calculated only from the multipath powers and directions. Since the powers and directional vectors are normalised to unity, the upper bound of any of the second order moments is equal to 0.5.

C. *Quantifying Directional Spread*

Since the second order moments R_{xx}, R_{yy}, R_{zz}, R_{xy}, R_{yz} and R_{zx} are directly related to the separation of directional vector components, $\sigma_\mathrm{m}^2(\hat{\mathbf{u}})$ can be expected to increase with the overall directional spread. $\sigma_\mathrm{m}^2(\hat{\mathbf{u}})$ can be calculated directly for any given multipath energy distribution using the results given in (9) and (10). However, $\sigma_\mathrm{m}^2(\hat{\mathbf{u}})$ has by definition a dependency on direction and for conciseness, a scalar quantity that includes the fading statistics over all spherical directions might be preferred instead. In this section a simple quantification of directional spread is proposed using an eigenvalue analysis of $(\nabla f)(\nabla f)^T$.

For a generic directional distribution of multipath power, the distribution of ∇f over the 3 euclidean co-ordinates as calculated for independent phase realisations of the multipath components takes the shape of an ellipsoid. The eigenvalue decomposition of the covariance matrix of ∇f is given by

$$\mathbf{R} = E\{(\nabla f)(\nabla f)^T\} = \begin{bmatrix} R_{xx} & R_{xy} & R_{zx} \\ R_{xy} & R_{yy} & R_{yx} \\ R_{zx} & R_{yz} & R_{zz} \end{bmatrix} = \mathbf{P}\Lambda\mathbf{P}^T \quad (12)$$

where Λ = diag{[λ_1 λ_2 λ_3]} and $\mathbf{P}$ = [$\mathbf{e}_1$ $\mathbf{e}_2$ $\mathbf{e}_3$]. The constituent basis vectors $\mathbf{e}_i$ give the principle directions of the ellipsoid. For $\lambda_1 > \lambda_2 > \lambda_3$, the vector $\mathbf{e}_1$ gives the direction of maximum stretch of the distribution of ∇f in the Euclidean space. The sum of eigenvalues of a correlation matrix is equivalent to its trace, as shown in (13).

$$\text{trace}(\mathbf{R}) = \lambda_1 + \lambda_2 + \lambda_3 = R_{xx} + R_{yy} + R_{zz} \quad (13)$$

Now, consider the mean of $\sigma_m^2(\hat{\mathbf{u}})$ over all 3-D angles. Random directional unit vectors that give uniformly distributed points on the surface of the sphere can be generated using numerous methods based on [12], where u_x, u_y and u_z are independent random variables uniformly distributed in the range [-1, 1]. Denoting their probability density functions as $p(u_x)$, $p(u_y)$ and $p(u_z)$, the mean is given by (14).

$$\begin{aligned} E\{\sigma_m^2(\hat{\mathbf{u}})\} &= R_{xx}E\{u_x^2\} + R_{yy}E\{u_y^2\} + R_{zz}E\{u_z^2\} + 2R_{xy}E\{u_x u_y\} + \\ &\quad + 2R_{yz}E\{u_y u_z\} + 2R_{zx}E\{u_z u_x\} \\ &= R_{xx}\int_{-1}^{1} u_x^2 p(u_x)du_x + R_{yy}\int_{-1}^{1} u_y^2 p(u_y)du_y + R_{zz}\int_{-1}^{1} u_z^2 p(u_z)du_z \\ &= \frac{1}{3}(R_{xx} + R_{yy} + R_{zz}) \end{aligned} \quad (14)$$

Thus, trace($\mathbf{R}$) gives a measure of the second order fading statistics averaged over all spherical directions and can be rewritten as

$$\begin{aligned} \text{trace}(\mathbf{R}) &= R_{xx} + R_{yy} + R_{zz} \\ &= \frac{1}{2}\sum_{s}^{N_S} A_s^2\left[(d_x - \bar{d}_x)^2 + (d_y - \bar{d}_y)^2 + (d_z - \bar{d}_z)^2\right] \\ &= \frac{1}{2}\sum_{s}^{N_S} A_s^2 D_s^2 \end{aligned} \quad (15)$$

where D_s represents the Euclidean distance between directional unit vectors $\mathbf{d}_s$ and the mean directional vector $\bar{\mathbf{d}}$. The theoretical upper bound of trace($\mathbf{R}$) is equal to 0.5. A similar expression was proposed as a measure of "multipath component separation" in [13], but a derivation showing its relation with small-scale fading or directional spread was not given.

Higher trace($\mathbf{R}$) or RMS angular spread do not automatically imply lower correlation between space-diversity antennas as there is a dependency on array orientation as well. The level of variation in second order fading statistics with direction is modelled by the determinant of the correlation matrix, which is equivalent to the product of the eigenvalues, as given by (16).

$$\det(\mathbf{R}) = \lambda_1 \lambda_2 \lambda_3 \quad (16)$$

The det($\mathbf{R}$) gives a measure of invariance of the second order fading statistics with direction. As $\mathbf{R}$ becomes more ill-conditioned, det($\mathbf{R}$) decreases and the variation in $\sigma_m^2(\hat{\mathbf{u}})$ with $\mathbf{u}$ increases. The theoretical upper bound of det($\mathbf{R}$) is achieved when the eigenvalues are equal and their summation equals 0.5, such that $\lambda_1\lambda_2\lambda_3 = (0.5/3)^3 = 0.0046$. This occurs when the distribution of multipath power is perfectly isotropic and variation in $\sigma_m^2(\mathbf{u})$ with $\mathbf{u}$ is zero. Trace($\mathbf{R}$) also achieves its upper bound in this scenario.

For multipath profiles comprising of only one directional cluster, both trace($\mathbf{R}$) and det($\mathbf{R}$) can be expected to improve with the directional spread. The importance of det($\mathbf{R}$) is highlighted by the case where the multipath distribution comprises only two rays approaching from directly opposite directions. Here, trace($\mathbf{R}$) and RMS angular spread achieve their upper bounds, but det($\mathbf{R}$) is equal to zero as the variation in $\sigma_m^2(\mathbf{u})$ with $\mathbf{u}$ is greatest. $\sigma_m^2(\hat{\mathbf{u}})$ is maximum when $\mathbf{u}$ is parallel to the line of the opposite rays, but zero when $\mathbf{u}$ is perpendicular to the rays implying perfectly correlated antennas for this orientation of a linear array. Hence, trace($\mathbf{R}$) and det($\mathbf{R}$) are both required for characterising the directional distribution, as they describe the average and the variation of $\sigma_m^2(\hat{\mathbf{u}})$ over the 3D directional space.

III. Simulation Results

A diagrammatical demonstration of the theory introduced in Section II is presented in this section. Generic directional distributions comprising of either one or two clusters of multipath components were constructed, as shown in Figure 1. For simplicity, the cluster energies were modelled to be uniformly distributed in the range of [-Γ/2, Γ/2] in the azimuth and [-Δ/2, Δ/2] in elevation, with clusters mean directions contained within the azimuth (or x-y) plane. For the two cluster distribution, the angular separation between the mean directions of the clusters was denoted as β.

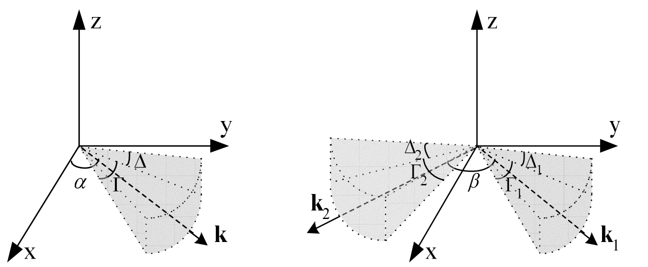

Figure 1: Multipath distributions comprising of one or two clusters and their parameters. The cluster means $\mathbf{k}_1$ and $\mathbf{k}_2$ are contained within the x-y plane.

1) Second order moments of fading: A validation for the derived expressions given in (9) and (10) was obtained by comparing them with their direct estimates, which were calculated using (4). The direct estimates were calculated from a large number of realisations of the partial derivatives (f_x, f_y,

f_z), which were obtained using distinct and independent multipath phase profiles. The multipath component phases within each profile were assumed to be random and uniformly distributed in $[0, 2\pi)$, as was suggested in [14]. A close match was found between the estimates and the derived equations, as shown in Figure 2.

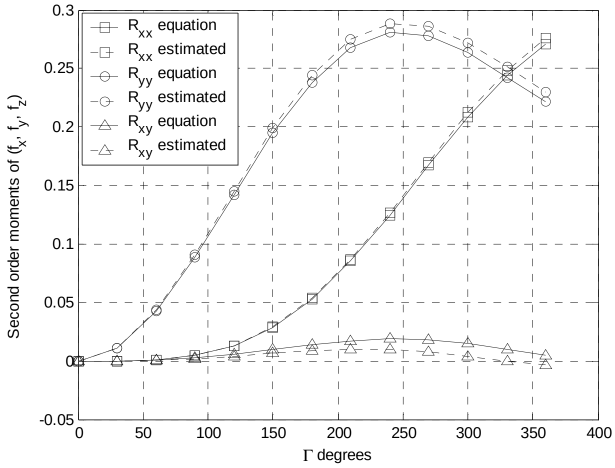

Figure 2: Second order moments of (f_x, f_y, f_z) against cluster azimuth width, for cluster mean direction **k** = [1,0,0] and elevation width $\Delta = 20°$. Dotted lines show estimates obtained using (4) and solid lines show results from (9) and (10).

The second order fading moments are a function of the mean cluster angle as well as the angular spread of the cluster. When the mean cluster direction is parallel to the x-axis, R_{yy} is larger than R_{xx} due to the greater separation between the directional vectors along the *y*-axis. As the cluster is rotated in the *x*-*y* plane, the second order fading moments are periodic as a function of the mean cluster angle, as shown in Figure 3.

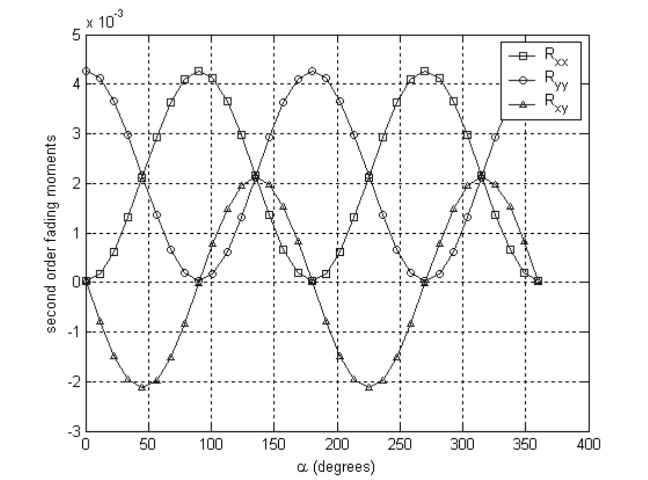

Figure 3: R_{xx}, R_{yy} and R_{xy} against mean cluster angle in azimuth.

The average R_{xx}, R_{yy} or R_{zz} of a uni-cluster multipath distribution increases with cluster angular width, as shown in Figure 4. This is expected as R_{xx} is equivalent to $\sigma_m^2(\mathbf{u})$ for $\mathbf{u} = [1,0,0]$.

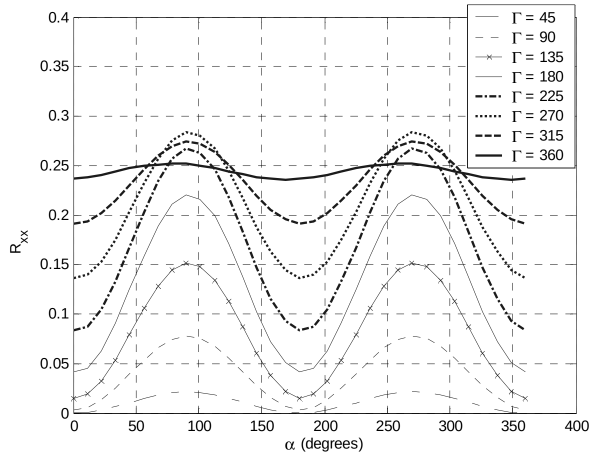

Figure 4: R_{xx} against cluster mean angle in the *x*-*y* plane, for a number of cluster azimuth widths and elevation width of $\Delta = 20°$.

2) Variance of Directional Derivative - $\sigma_m^2(\hat{\mathbf{u}})$: For a given directional energy profile $p(\theta, \varphi)$, $\sigma_m^2(\hat{\mathbf{u}})$ gives a measure of decorrelation between elements of a ULA as a function of its orientation, where the line of the array is given by **u**. Figure 5 shows for the case of a single dominant cluster that $\sigma_m^2(\hat{\mathbf{u}})$ will be maximum when the angular separation between the mean cluster direction and **u** is 90º. This is in agreement with experimental studies where higher capacities were observed when the broadside of a linear array was perpendicular to the direction of the LOS component [15][16]. This also explains why RMS angular spread on its own is insufficient, as correlation of a space-diversity array varies with its orientation relative to the direction of the cluster.

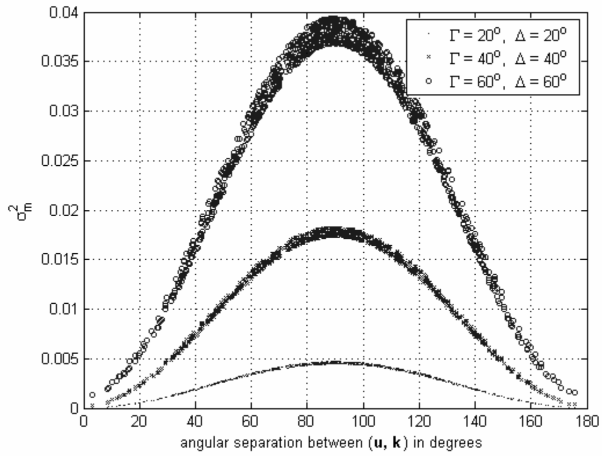

Figure 5. $\sigma_m^2(\mathbf{u})$ against angular separation of vectors **u** and **k,** for different angular spreads of a cluster.

Now consider the case where multipath energy arrives in two identically distributed clusters from different directions. Here, R_{xx}, R_{yy} and R_{zz} vary periodically with the overall rotation of the clusters, similar to that shown for the single cluster case in Figure 3. R_{xx} approaches its maximum value of 0.5 when two clusters are incident from opposite ends of the x-axis and the cluster widths tend towards zero. The general increase in $\sigma_m^2(\mathbf{u})$ with cluster angular separation is shown for two constituent cluster azimuth widths in Figure 6 and Figure 7. At $\beta = \pi$, $\sigma_m^2(\mathbf{u})$ is maximum when **u** is parallel to the line of the opposite clusters and minimum when it is perpendicular. Here, $\sigma_m^2(\mathbf{u})$ approaches its upper bound of 0.5 as the constituent cluster angular widths tend to zero. Note that this is in contrast to the single cluster case shown in Figure 5, where the direction of maximum fading is orthogonal to the mean cluster angle. A comparison between Figure 6 and Figure 7 demonstrates that the variation in $\sigma_m^2(\mathbf{u})$ with **u** decreases as the constituent cluster angular spreads are increased.

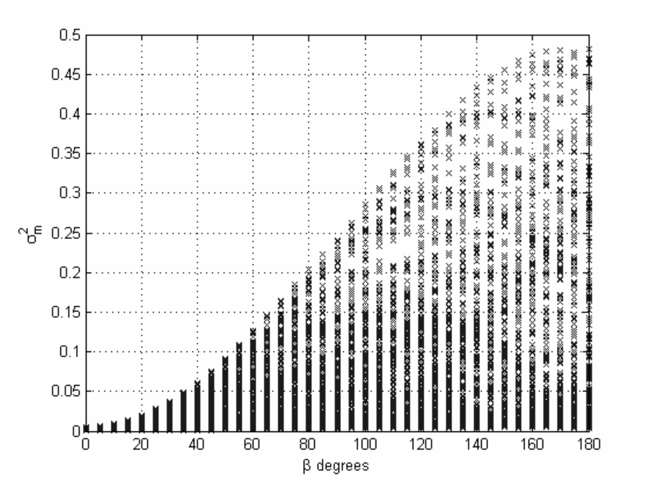

Figure 6: Distribution of $\sigma_m^2(\mathbf{u})$ for a bi-cluster multipath distribution, calculated for random and uniformly distributed spherical directions **u,** and $\Gamma_1 = \Gamma_2 = 20°$, $\Delta_1 = \Delta_2 = 20°$.

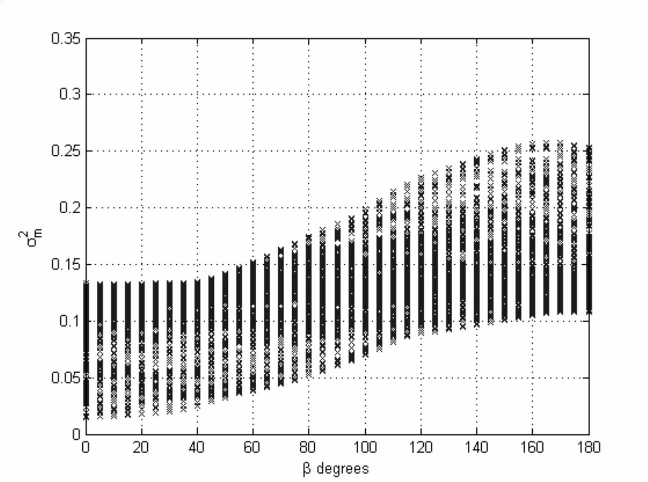

Figure 7: Distribution of $\sigma_m^2(\mathbf{u})$ for a bi-cluster multipath distribution, calculated for random and uniformly distributed spherical directions **u,** and $\Gamma_1 = \Gamma_2 = 120°$, $\Delta_1 = \Delta_2 = 20°$.

2) Directional Spread: The dependence of trace(**R**) and det(**R**) on the joint azimuth and elevation angular spreads are shown in Figure 8 and Figure 9 respectively. The results demonstrate that larger azimuth and elevation widths of a cluster lead to greater average fading over all directions, as given by trace(**R**), as well as lower variation in second order fading statistics with direction, as given by det(**R**).

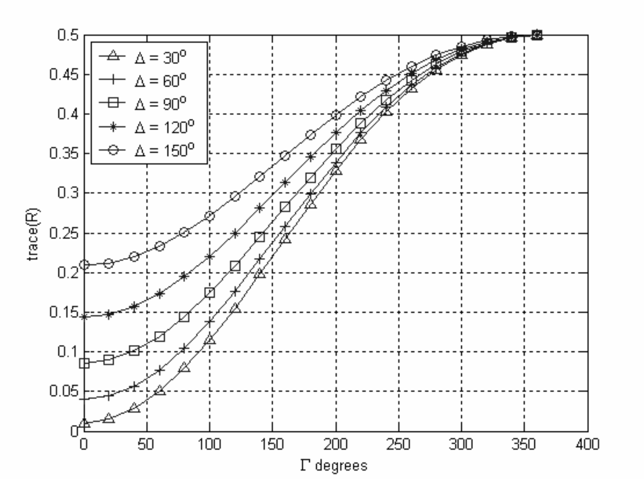

Figure 8. trace(**R**) of a cluster for different azimuth (Γ) and elevation (Δ) spreads.

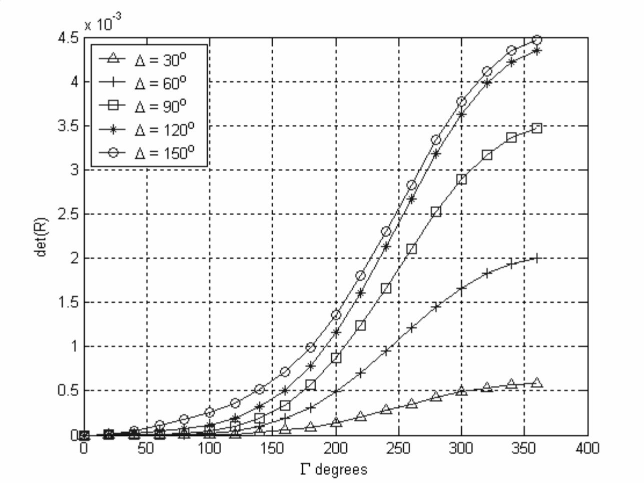

Figure 9. det(**R**) of a cluster for different Γ and Δ.

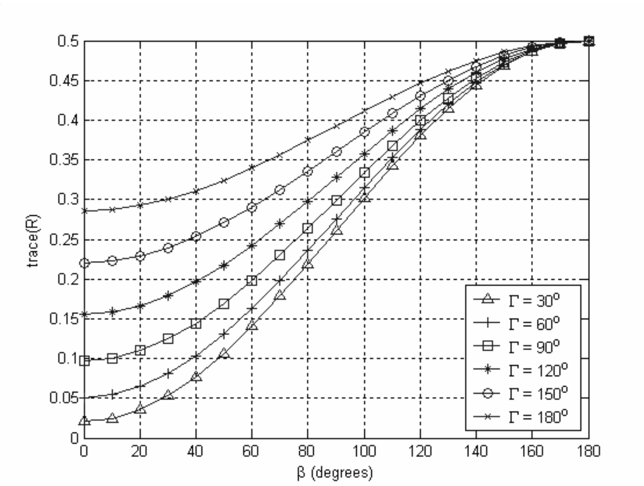

Figure 10. trace(**R**) against angular separation of 2 clusters, for Δ = 30º.

For the two cluster case, trace(**R**) achieves its maximum value of 0.5 when $\beta = \pi$ regardless of angular widths of the clusters (see Figure 10). However, det(**R**) continues to improve with the cluster angular spreads, as shown in Figure 11. This further highlights the importance of det(**R**) as a property of the directional distribution.

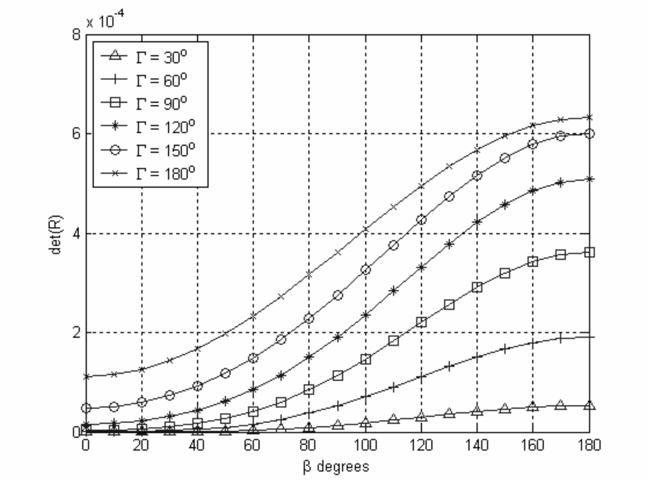

Figure 11. det(**R**) against angular separation of 2 clusters, for Δ = 30º.

3) Effect of K-factor: It is known that a dominant component reduces the fading in the channel and leads to a decrease in RMS angular spread. Figure 12 and Figure 13 show the variation in trace(**R**) and det(**R**) respectively with *K-factor* for a range of cluster azimuth and elevation spreads. High *K-factors* limit the directional spread, but the contrary is not true as lower *K-factors* do not necessarily lead to larger directional spreads. Thus, the use of *K-factor* as a measure of directional spread or multipath richness is incorrect.

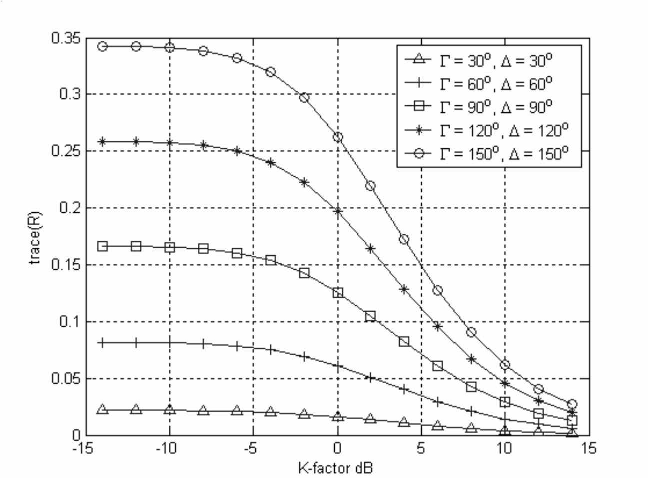

Figure 12. Variation in trace(**R**) with ricean *K-factor* for various Γ and Δ.

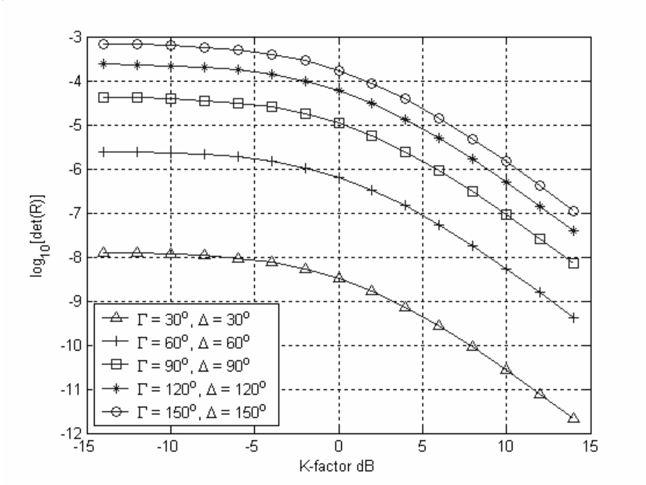

Figure 13. Variation in trace(**R**) with ricean *K-factor* for various Γ and Δ.

4) Analysis of ray-tracing data: The proposed metrics were used to analyse multipath component data that was obtained from a validated ray-tracing simulation of an open-plan office. Multipath profiles were obtained for over 4000 locations of the receiver and a fixed location of the transmitter. The heights of the transmitter and receiver were approximately 1 m. The correlations between the proposed directional spread metrics and the channel Pathloss, Cross-Polarization Coupling (XPC), *K-factor* and RMS delay spread (r.m.s DS) are summarised in Table 1. The correlations were calculated over all channel locations.

	trace(**R**)		log_{10}[det(**R**)]	
	(Tx)	(Rx)	(Tx)	(Rx)
XPC (dB)	0.70	0.60	0.47	0.50
Pathloss (dB)	0.65	0.49	0.44	0.46
K-factor (dB)	-0.35	-0.25	-0.30	-0.35
r.m.s DS	0.70	0.43	0.52	0.39

Table 1. Correlation coefficients between channel parameters

As expected, trace(**R**) and det(**R**) are positively correlated with channel XPC and Pathloss. Directional spread increases with rich scattering, which also causes multipath depolarization or coupling between orthogonal polarisations of a path. This is in direct contrast with LOS scenarios where pathloss is small and the orthogonal polarizations of the dominant path remain independent. Correlation between *K-factor* and directional spread is weaker as small *K-factors* do not necessarily lead to large directional spreads.

APPENDIX A.

A derivation of the general expression for the second order moment of the partial derivatives is shown here. The mean of f_x (or f_y, f_z) over a large number of phase realizations is equal to zero. Note that the amplitudes and directions are treated as constants, and the phases as random variables. Using (4) and (8), R_{xy} can be expressed as shown in (17).

$$
\begin{aligned}
R_{xy} &= E\{f_x f_y\} \\
&= E\left\{\sum_{s=1}^{N_s}\sum_{k=1}^{s} A_s A_k \left(d_{x_s} - d_{x_k}\right)\sin(\psi_s - \psi_k)\sum_{i=1}^{N_s}\sum_{j=1}^{i} A_i A_j \left(d_{y_i} - d_{y_j}\right)\sin(\psi_i - \psi_j)\right\} \\
&= E\left\{\sum_{s=1}^{N_s}\sum_{k=1}^{s}\sum_{i=1}^{N_s}\sum_{j=1}^{i} A_s A_k A_i A_j \left(d_{x_s} - d_{x_k}\right)\left(d_{y_i} - d_{y_j}\right)\sin(\psi_s - \psi_k)\sin(\psi_i - \psi_j)\right\}
\end{aligned}
\tag{17}
$$

The above mean can be assumed to be zero for summation terms with $(s,k) \neq (i,j)$ and will be computed only for $(s,k) = (i,j)$, as shown in (18).

$$
\begin{aligned}
R_{xy} &= E\left\{\sum_{s=1}^{N_s}\sum_{k=1}^{s} A_s^2 A_k^2 \left(d_{x_s} - d_{x_k}\right)\left(d_{y_s} - d_{y_k}\right)\sin^2(\psi_s - \psi_k)\right\} \\
&= \sum_{s=1}^{N_s}\sum_{k=1}^{s} A_s^2 A_k^2 \left(d_{x_s} - d_{x_k}\right)\left(d_{y_i} - d_{y_j}\right) E\left\{\sin^2(\psi_s - \psi_k)\right\}
\end{aligned}
\tag{18}
$$

Without loss of generality, the second order moment of fading derivative can be described at a point **s** = [0, 0, 0]. The phase term ψ_s simplifies to just the random phase component χ_s (see (5)). Assuming χ_s to be random and uniformly distributed in $[0\ 2\pi)$, the variance term is given by

$$
\mathrm{var}\{\sin(\psi_s - \psi_k)\} = \mathrm{var}\{\sin(\phi)\} = \int_0^{2\pi} \sin^2(\phi)\,\mathrm{d}\phi = \frac{1}{2} \tag{19}
$$

where the random variable ϕ can be expected to be uniformly distributed in $[0, 2\pi)$. Using (19), the result in (18) further simplifies to that in (20).

$$
R_{xy} = \frac{1}{2}\sum_{s=1}^{N_s}\sum_{k=1}^{s} A_s^2 A_k^2 \left(d_{x_s} - d_{x_k}\right)\left(d_{y_s} - d_{y_k}\right) \tag{20}
$$

The equivalence between the expressions for R_{xy} given in (20) and (9) is demonstrated by the fact that they both simplify to the same result, as shown in (21) and (22) respectively.

$$
\begin{aligned}
R_{xy} &= \frac{1}{2}\sum_{s=1}^{N_s}\sum_{k=1}^{s} A_s^2 A_k^2 \left(d_{x_s} - d_{x_k}\right)\left(d_{y_s} - d_{y_k}\right) \\
&= \frac{1}{4}\sum_{s=1}^{N_s}\sum_{k=1}^{N_s} A_s^2 A_k^2 \left(d_{x_s} - d_{x_k}\right)\left(d_{y_s} - d_{y_k}\right) \\
&= \frac{1}{4}\Bigg[\sum_{s=1}^{N_s} A_s^2 d_{x_s} \sum_{k=1}^{N_s} A_k^2 d_{y_k} + \sum_{s=1}^{N_s} A_s^2 d_{y_s} \sum_{k=1}^{N_s} A_k^2 d_{x_k} \\
&\quad - \sum_{s=1}^{N_s} A_s^2 d_{x_s} d_{y_s} \sum_{k=1}^{N_s} A_k^2 - \sum_{s=1}^{N_s} A_s^2 \sum_{k=1}^{N_s} A_k^2 d_{x_k} d_{y_k}\Bigg] \\
&= \frac{1}{2}\bar{d}_x \bar{d}_y - \frac{1}{2}\sum_{s=1}^{N_s} A_s^2 d_{x_s} d_{y_s}
\end{aligned}
\tag{21}
$$

$$
\begin{aligned}
R_{xy} &= \frac{1}{2}\sum_{s=1}^{N_s} A_s^2 \left(d_{x_s} - \bar{d}_x\right)\left(d_{y_s} - \bar{d}_y\right) \\
&= \frac{1}{2}\sum_{s=1}^{N_s} A_s^2 d_{x_s} d_{y_s} + \frac{1}{2}\sum_{s=1}^{N_s} A_s^2 \left(\sum_{k=1}^{N_s} A_k^2 d_{x_k}\right)\left(\sum_{k=1}^{N_s} A_k^2 d_{y_k}\right) + \\
&\quad - \frac{1}{2}\sum_{s=1}^{N_s} A_s^2 d_{x_s} \sum_{k=1}^{N_s} A_k^2 d_{y_k} - \frac{1}{2}\sum_{s=1}^{N_s} A_s^2 d_{y_s} \sum_{k=1}^{N_s} A_k^2 d_{x_k} \\
&= \frac{1}{2}\sum_{s=1}^{N_s} A_s^2 d_{x_s} d_{y_s} + \frac{1}{2}\sum_{k=1}^{N_s} A_k^2 d_{x_k} \sum_{k=1}^{N_s} A_k^2 d_{y_k} \sum_{s=1}^{N_s} A_s^2 - \bar{d}_x \bar{d}_y \\
&= \frac{1}{2}\sum_{s=1}^{N_s} A_s^2 d_{x_s} d_{y_s} - \frac{1}{2}\bar{d}_x \bar{d}_y
\end{aligned}
\tag{22}
$$

REFERENCES

[1] T. S. Rappaport, *Wireless Communications: Principles and Practice*. Englewood Cliffs, NJ: Prentice-Hall 1996.

[2] R. M. Buehrer, "The Impact of Angular Energy Distribution on Spatial Correlation", VTC 2002-Fall IEEE 56th Proceedings, pp. 1173 - 1177 vol.2, Sept. 2002.

[3] K. Yu, Q. Li and M. Ho, "Measurement Investigation of Tap and Cluster Angular Spreads at 5.2 GHz", *IEEE Transaction on Antennas and Propagation*, vol. 53, issue 7, pp. 2156- 2160, July 2005.

[4] G. D. Durgin and T. S. Rappaport, "Theory of Multipath Shape Factors for Small-Scale Fading Wireless Channels," *IEEE Transactions on Antennas and Propagation*, vol. 48, no. 5, pp. 682–693, May 2000.

[5] M. Patzold, "System Function and Characteristic Quantities of Spatial Deterministic Gaussian Uncorrelated Scattering Processes", *IEEE VTC Spring 2003*, vol.1, pp. 256-261, April 2003.

[6] T. Svantesson and J. W.0 Wallace, "On Signal Strength and Multipath Richness in Multi-Input Multi-Output Systems", *IEEE International Conference on Communications,* ICC '03, Vol. 4, pp. 2683-2687, 2003.

[7] M. Steinbauer, A. F Molisch, and E. Bonek, "The Double-Directional Radio Channel," *IEEE Antennas and Propagation Magazine*, vol. 43, pp. 51–63, Aug. 2001.

[8] J. P. Kermoal, P. E. Mogensen, S. H. Jensen, J. B. Andersen, F. Frederiksen, T. B. Sørensen, and K. I. Pedersen, "Experimental Investigation of Multipath Richness for Multi-Element Transmit and Receive Antenna Arrays", *IEEE VTC 2000 Spring, Tokyo, Japan, vol.3*, pp. 2004-2008, May 2000.

[9] D-S. Shiu, G. J. Foschini, M. J. Gans, and J. M. Kahn, "Fading Correlation and its effect on the Capacity of Multi-Element Antenna Systems", *IEEE International conference on Universal personal communications* (ICUPC'98), vol. 1, pp. 429–433, October 1998.

[10] J. W. Wallace, M. A. Jensen, "MIMO Capacity Variation with SNR and Multipath Richness from Full-wave Indoor FDTD Simulations", Antennas and Propagation Society International Symposium, vol. 2, pp 523 – 526, June 2003.

[11] J. B. Andersen and J. Ø. Nielsen, "Multipath Richness – a Measure of MIMO Capacity in an Environment", *COST 273*, TD (04) 157, Duisberg, September 2004.

[12] G. Marsaglia, "Choosing a point from the surface of a sphere", The Annals of Mathematical Statistics, 43, pp. 645-646, 1972.

[13] M. Steinbauer, H. Özcelik, H. Hofstetter, C. F. Mecklenbräuker and E. Bonek, "How to Quantify Multipath Separation", *IEICE Trans. Electron., Special Issue*, vol.E85-C, no. 3, pp. 552-557, 2002.

[14] A. F. Molisch, M. Steinbauer, M. Toeltsch, E. Bonek, and R. S. Thoma, "Capacity of MIMO systems based on measured wireless channels", *IEEE JSAC.*, vol. 20, pp. 561–569, April 2002.

[15] P. Almers, F. Tufvesson, P. Karlsson and A. F. Molisch, "The Effect of Horizontal Array Orientation on MIMO Channel Capacity", Proceedings of IEEE Vehicular Technology Conference, April 2003.

[16] D. P. McNamara, "Characterisation and Investigation of Multiple Input Multiple Output Wireless Communication Channels", Chapter 4, Ph.D. Thesis, Faculty of Engineering, University of Bristol, March 2003.